JOURNAL OF AIRCRAFT
Vol. 38, No. 3, May–June 2001

Preliminary Results of BE-1900D Operational Flight Loads Data Evaluation

Thomas A. Zeiler*
University of Alabama, Tuscaloosa, Alabama 35405
and
Daniel O. Tipps,† Donald A. Skinn,‡ and John W. Rustenburg§
University of Dayton Research Institute, Dayton, Ohio 45469

The preliminary results of a statistical analysis of flight loads data from BE-1900D twin-engine turboprop aircraft in normal commuter transport operations are presented. Some details of data-reduction procedures are discussed, and flight loads data are presented in statistical formats and discussed. Although these data are preliminary, they suggest that loading spectra typically used in design are generally more severe than those derived from the present data. An exception to this general result is at the lower levels of incremental maneuver load factor. Some results also suggest that there are circumstances in which aircraft are being flown at speeds in excess of required limits. Some issues related to quality and completeness of recorded data are discussed. Recommendations for improvement of future data gathering activities are made.

Nomenclature

A_r	=	aspect ratio b^2/S
a	=	speed of sound, ft/s
a_0	=	speed of sound at sea level, ft/s
b	=	wing span, ft
$\bar{C}$	=	aircraft discrete gust response factor
C_{L_α}	=	wing lift curve slope per radian
$\bar{c}$	=	wing mean geometric chord, ft
D	=	distance
g	=	gravity constant, 32.17 ft/s^2
H_p	=	pressure altitude, ft
K	=	gust alleviation constant
K_g	=	discrete gust alleviation factor, $0.88\,\mu/(5.3+\mu)$
M	=	Mach number
m	=	lift curve slope per radian
n	=	load factor, g
n_z	=	normal load factor, g
q	=	dynamic pressure, lb/ft^2
S	=	wing area, ft^2
U_{de}	=	derived gust velocity, ft/s
V_e	=	equivalent airspeed
V_T	=	true airspeed
W	=	gross weight, lb
μ	=	aircraft mass ratio, $2W/\rho g \bar{c} C_{L_\alpha} S$
ρ	=	air density, slug/ft^3, at pressure altitude (H_p), from Eq. (3)

Introduction

DURING the decade of the 1990s, there was a strong interest worldwide in characterizing the actual loading environment experienced by aircraft in typical operations.[1–8] Most attention to date has been given to large transport aircraft,[4,6–8] though there has been some data collected for special situations[2] and general aviation aircraft.[3] Until recently[9] there has been little loads data collected for a rapidly growing segment of operational flight operations, namely, commuter operations. Commuter carriers have been in operation for a long time. However, it is only recently that the market share of these operations has begun to grow substantially as air carriers centralize large transport operations at hub airports, relying on commuter operations to "feed" passengers from outlying areas to these central operations hubs. Thus it is important that the Federal Aviation Administration (FAA), and the aviation community at large, have a picture of the loads environment encountered in commuter operations.

This paper summarizes the preliminary statistical loads data for commuter operations presented in Ref. 9. The data were collected from digital flight data recorders (DFDRs) on 28 Beech BE-1900D turboprop aircraft, a Part 23 aircraft (Fig. 1 and Table 1),[10] representing 903 flights and approximately 585 hours of operation. Flight and ground loads data, aircraft usage data, and engine data were collected and analyzed (Table 2), but only the flight loads data are presented in this paper. Because of the relatively small number of aircraft and flight hours and the fact that the operations were over a limited region of the United States, the load statistics may not be stabilized. However, it is the first such data collected for commuter operations in the United States. Efforts at acquiring more flight data are continuing.

Data Reduction

Data Collection and Editing

A solicitation by the FAA for participation in operational loads monitoring of BE-1900D aircraft was answered by an operator who was downloading DFDR data for its own purposes, but needed help in statistically collating and analyzing the data being obtained. An agreement was made wherein the DFDR data would be analyzed under an existing FAA grant and small recording devices would be installed on several of the aircraft to obtain selected data over a longer term than the DFDR data represented. The airline ground data editing station performed a number of functions during the process of transferring the raw flight data into DOS file formats and onto hard disks. The two most important functions were an integrity check of the data and removal of flight sensitive information. The aircraft operator removed all sensitive information and forwarded the desensitized data for processing and analysis.

All of the parameters listed in Table 2 except pitch control were used for statistical analysis and data presentation. Pitch control is the measure of the control yoke in the fore and aft direction and indicates the amount of elevator deflection being input by the pilot.

Received 19 January 2000; revision received 20 September 2000; accepted for publication 22 September 2000.

*Assistant Professor, Aerospace Engineering and Mechanics Department. Senior Member AIAA.
†Research Engineer/Group Leader Flight Systems Integrity.
‡Associate Research Programmer/Flight Loads.
§Research Engineer/Flight Loads.

Table 1 BE-1900D aircraft characteristics[10]

Parameter	Value
Maximum taxi weight	17,060 lb
Maximum takeoff weight	16,950 lb
Maximum landing weight	16,600 lb
Zero-fuel weight	15,000 lb[a]
Fuel capacity	668 U.S. gallons
2 P&W PT6A-67D turboprops	@ 1,279 shp each
Wing span	57 ft 11.25 in.
Wing reference area	310 ft^2
Wing MAC	5.32 ft
Length	57 ft 10 in.
Height	15 ft 6 in.
Tread	17 ft 2 in.
Wheel base	23 ft 9.5 in.

[a] Operator provided an "empty weight" of 10,350 lbs.

Table 2 Recorded flight and loads parameters

Parameter	Sample rate per second
Normal acceleration, g	8
Longitudinal acceleration, g	4
Flap position (L&R), discrete	1
Pitch control, deg	2
RPM L, rpm	1
RPM R, rpm	1
Prop. reverse (L&R), discrete	1
Indicated airspeed, kn	1
Pressure altitude, ft	1
Bank angle, deg	2
Pitch angle, deg	2
Magnetic heading, deg	1
Torque L, ft-lb	1
Torque R, ft-lb	1

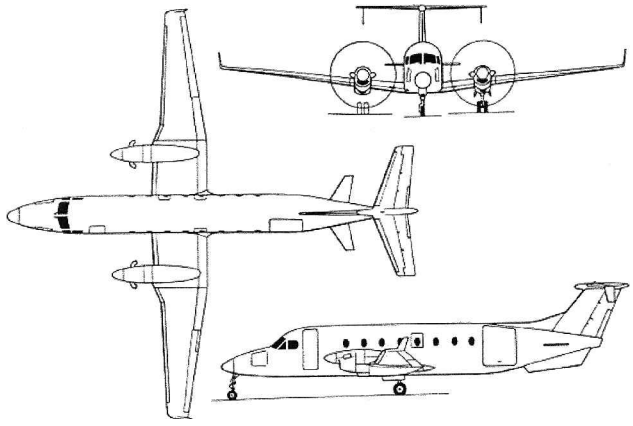

Fig. 1 BE-1900D three view.[10]

Measurements of pilot input to cable driven systems do not accurately relate to the actual position of the elevator during flight as a result of cable stretch. Thus, because of the questionable accuracy these data were not processed.

All data files were initially screened for missing or incomplete data before being accepted for statistical analysis. Individual flights were edited to remove erroneous or meaningless data such as discontinuous elapsed time data, evidence of nonfunctional channels or sensors, multiple flights on one file, and incomplete flight phases. Flight files with missing or incomplete data were rejected.

Derived and Extracted Parameters

Certain information and parameters needed in the data reduction were not recorded and needed to be either extracted or derived from the available time history data. Some of these parameters had to be calculated. For example, the lift curve slopes were not available from the aircraft manufacturer. Because gross weight was not a recorded parameter, a 45-day average takeoff weight of 14,500 lb provided by the aircraft operator or the maximum gross weight of 16,950 lb was used in calculations that required weight.

Table 3 Phase of flight starting criteria

Phase of flight	Conditions at start of phase
Taxi out	Initial condition
Takeoff roll	Computed airspeed >45 kns or n_x >0.15 g
Departure	Time at liftoff; flaps extended
Climb	Flaps retracted; rate of climb $\geq$ 750 ft/min for at least 20 s
Cruise	Flaps retracted; rate of climb $\leq$ 750 ft/min for at least 20 s
Descent	Flaps retracted; rate of descent $\geq$ 750 ft/min for at least 20 s
Approach	Flaps extended
Landing roll	Touchdown
Taxi in	Magnetic heading change greater than 13.5 deg after touchdown

Each flight was divided into nine phases: four ground phases (taxi out, takeoff roll, landing roll, and taxi in) and five airborne phases (departure, climb, cruise, descent, and approach). Table 3 lists the conditions for determining the starting times for each phase. An airborne phase can occur several times per flight because it is determined by the rate of climb and the position of the flaps. When this occurs, the flight loads data are combined and presented in a single flight phase.

In the absence of a squat switch, the approximate time of liftoff and touchdown was determined by an algorithm that used time history information of pitch angle, vertical and longitudinal accelerations, and changes in altitude and indicated airspeed. The actual time at liftoff is determined by calculating the average pitch angle while the aircraft is on the ground. Then, the point in time when the pitch angle changes by more than 2 deg from this average is defined as the time of liftoff. The time of touchdown was selected by using the best combination of when the pitch angle, vertical and longitudinal accelerations, airspeed, and altitude indicated that contact with the runway had occurred. The flight duration is defined as the time from aircraft liftoff to touchdown. The criterion for defining the start of the takeoff roll is the earlier of 1) the time that the indicated speed exceeds 45 kn or 2) the time that the longitudinal acceleration exceeds 0.15 g prior to liftoff.

The criterion for defining the start of taxi in is the time when the aircraft turns off the active runway. The method for detecting turn off is to monitor magnetic heading for a change greater than 13.5 deg from the landing magnetic heading. The time when the heading starts to change in the turn off direction is then identified as the start of the turn or the beginning of the taxi in phase. This method can, however, fail to detect a shallow turn off onto a parallel taxiway. In this case an average landing roll of 32 s duration is assumed and the turn off is marked as 32 s after touchdown.

The peak-between-means method[11] was used to select the peaks and valleys in the acceleration data. This method is consistent with past practices and pertains to all accelerations (n_x, Δn_z, $\Delta n_{z_{\text{man}}}$, $\Delta n_{z_{\text{gust}}}$). This method counts upward events as positive and downward events as negative. Only one peak or one valley is counted between two successive crossings of the mean. A threshold zone (dead band) is used in the data reduction to ignore small variations about the mean. For the normal accelerations Δn_z the threshold zone is ± 0.05 g; for longitudinal accelerations n_x the threshold zone is ± 0.005 g.

The incremental acceleration measured near the c.g. of the aircraft may be the result of either maneuvers or gusts. The accelerometers used by the flight data recorder are near the true c.g of the vehicle. Though the true c.g. actually moves from one loading condition to another and as fuel is consumed the variation is sufficiently small, as is the error in accelerometer position, only unreasonably high angular accelerations would be needed to introduce significant

Table 4 Absolute pressure altitude bands

Band	Distance, ft
1	<500
2	501–1,500
3	1,501–4,500
4	4,501–9,500
5	9,501–14,500
6	14,501–19,500
7	19,501–24,500

error between the recorded accelerations and the actual c.g. accelerations. To derive gust and maneuver statistics, the maneuver-induced acceleration and gust-response accelerations must be separated from the total acceleration history. As a result of Ref. 12, it was recommended and accepted by the FAA that a cycle-duration rule be used to separate gusts and maneuvers. A cycle duration of 2.0 s was recommended for use with B-737 and MD-82/83 aircraft. Review of the BE-1900D response characteristics has shown that this cycle duration can also be used with the BE-1900D data. To avoid the inclusion of peaks and valleys associated with very small load variations that are insignificant to the aircraft structure, a threshold zone of $\Delta n_z = \pm 0.05$ g was established. An algorithm was then developed to extract the acceleration peaks and valleys. As a result of the threshold zone, only accelerations greater than ± 0.05 g (measured from a 1.0-g base) are counted for data presentation. For a flight any bias occurring in the vertical (i.e., normal) acceleration measurement is removed by adjusting the difference between a known 1-g level and the actual acceleration recorded value. This difference is the correction/bias that will be added/subtracted from all measured load factor values for the flight.

In Ref. 6 some data for the departure and approach phases of flight were sorted according to altitude above the departure or arrival airports, respectively. For the data presented in this paper, only the absolute pressure altitude (a recorded parameter) is pertinent. The pressure altitude bands shown in Table 4 were used.

The flight distance D is obtained by numerically integrating true velocity V_T from the time of liftoff t_0 to the time of touchdown t_n. If V_T is the average true airspeed during the time increment Δt, then

$$D = \sum_{t_0}^{t_n} \Delta t \cdot V_T \tag{1}$$

This computation does not give actual geometric distance, but rather the amount of air that the vehicle is flown through (e.g., "air miles"). For a perfect speed indicator the indicated airspeed equals the calibrated airspeed. In this report the indicated airspeed is assumed to equal the calibrated airspeed. Assuming incompressible flow and neglecting the small effects at low Mach numbers, the true airspeed can be found as

$$V_T \approx V_C \sqrt{\rho_0/\rho} \tag{2}$$

where ρ_0 is air density at sea level (0.0023769 slugs/ft^3). For altitudes below 36,089 ft the density is expressed as a function of altitude based on the International Standard Atmosphere by

$$\rho = \rho_0 (1 - 6.876 \times 10^{-6} \times H_p)^{4.256} \tag{3}$$

Flight Data

The gust loads data are presented as cumulative occurrences of vertical gust load factor and as cumulative occurrences of derived gust velocity. Gust load factor data are also compared with recorded data from other aircraft types and with other published data. Figure 2 presents the cumulative occurrences of incremental vertical gust

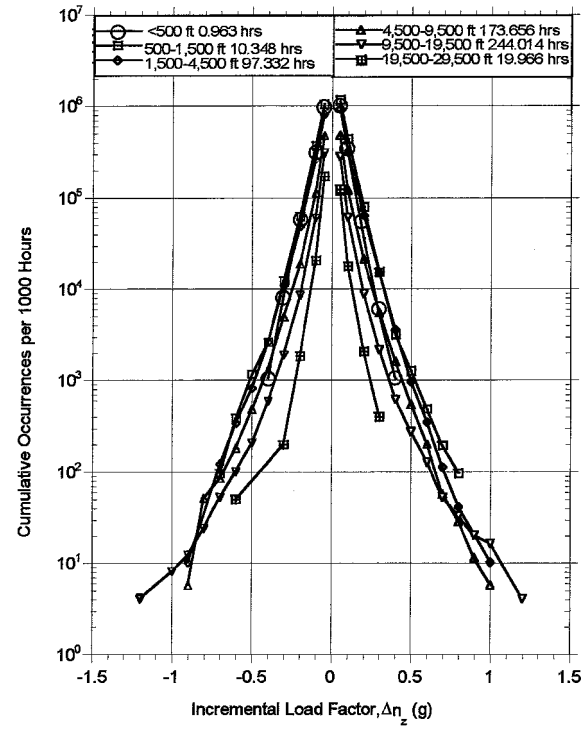

Fig. 2 Cumulative occurrences of incremental gust load factor per 1000 hours by pressure altitude (combined climb, cruise, and descent phases).

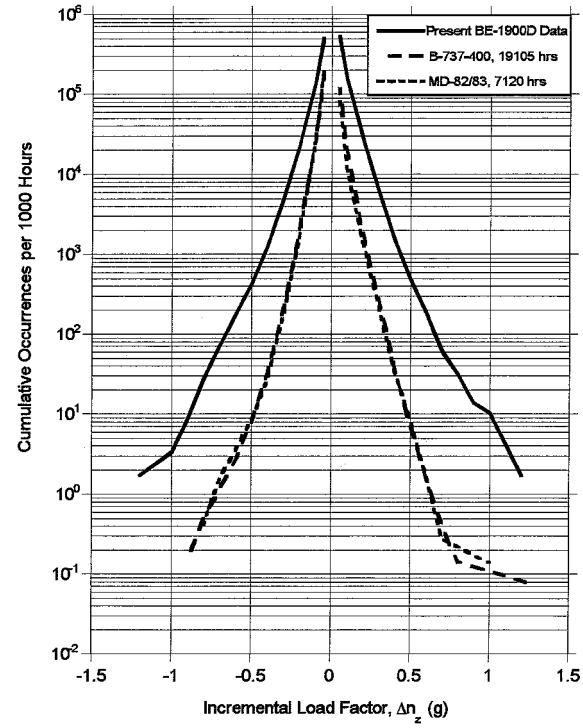

Fig. 3 Cumulative occurrences of incremental gust load factor per 1000 hours, present data, B-737-400, MD-82/83 (combined flight phases).

load factor per 1000 hours by pressure altitude for the combined climb, cruise, and descent phases of flight. Figure 3 shows the difference in severity of vertical load factor for gust between a commuter aircraft, the BE-1900D, and two large transport aircraft, the B-737 and the MD82/83 during routine commercial operations, obtained from Refs. 4, 6, and 7. The BE-1900D aircraft load factor response to gust is more than twice the severity of the B-737. It was found that the difference in responses is largely accounted for by an analysis

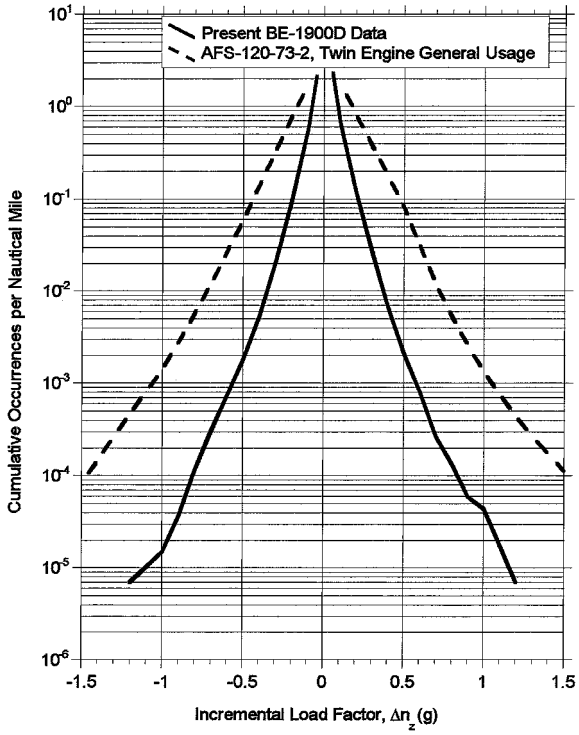

Fig. 4 Cumulative occurrences of incremental gust load factor per nautical mile, present data and AFS-120-73-2, (combined flight phases).

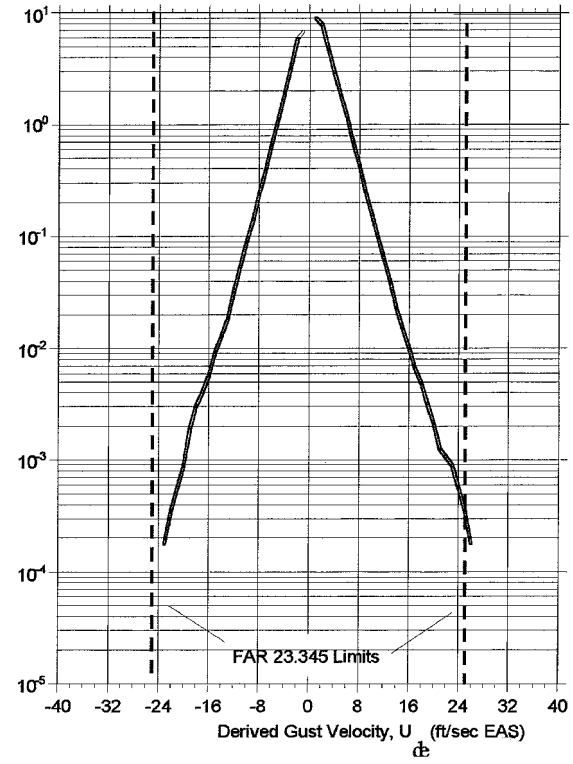

Fig. 5 Cumulative occurrences of derived gust velocity per nautical mile for flap extended.

of the aircraft discrete gust response factor (see the following). The wing loading of the BE-1900D is roughly twice that of the large transports. Also, the BE-1900D operates at lower altitudes where turbulence is more severe.

The gust and maneuver load spectra specified in Ref .13 are expressed in terms of the ratio of the incremental load factor at operating weight to the incremental design limit load factor at maximum gross weight. Therefore, in order to compare the BE-1900D gust and maneuver flight load factor spectra with the Ref. 13 flight load spectra the aircraft design limit load factor for both gust and maneuver had to be estimated. To compare gust spectra, the incremental gust design limit load factor was calculated as specified in Ref. 13 using the maximum gross weight of 16,950 lb. Figure 4 shows that the twin-engine general spectra for gust is more severe than the present BE-1900D spectra.

The derived gust velocity, U_{de} was computed from the measured gust acceleration data using

$$U_{\text{de}} = \Delta n_z / \bar{C} \tag{4}$$

where Δn_z is gust peak incremental normal acceleration and $\bar{C}$ is the aircraft response factor considering the plunge-only degree of freedom and is calculated from

$$\bar{C} = \frac{\rho_0 V_e C_{L_\alpha} S}{2W} K_g \tag{5}$$

For this study the wing lift curve slope was obtained from the one-dimensional approximation[14] given by

$$C_{l_\alpha} = \frac{2\pi A_r}{2 + \left[4 + A_r^2 \beta^2 (1 + \tan^2 \Lambda / \beta^2)\right]^{\frac{1}{2}}} \tag{6}$$

where $\beta = \sqrt{(1 - M^2)}$ and Λ is the quarter chord sweep angle. Mach number is derived from true airspeed and speed of sound a:

$$M = V_T / a \tag{7}$$

The speed of sound a is a function of pressure altitude H_p and the speed of sound at sea level and is

$$a = a_0 \sqrt{(1 - 6.876 \times 10^{-6} \times H_p)} \tag{8}$$

thus

$$M = V_T \Big/ a_0 \sqrt{(1 - 6.876 \times 10^{-6} \times H_p)}$$

where the speed of sound at sea level a_0 is 1116.4 fps or 661.5 kn. Equation (6) provides an estimate of the wing lift curve slope. Airplane gust-response calculations are based on the use of the airplane lift curve slope. Reference 15 suggests using an average factor of 1.15 to represent the ratio between the airplane lift curve slope and the wing lift curve slope. Therefore, the estimated wing lift curve slope values were multiplied by 1.15.

Figure 5 shows the cumulative occurrences of derived gust velocity per nautical mile (flight distance) with the flaps extended. The average takeoff gross weight of 14,500 lb was used in these calculations. Even with only 903 flight hours of data, the plot shows there are a few occurrences of derived gust velocity that exceed the FAR 23.345 requirement of 25 ft/s. Comparisons, not shown in this paper, of the derived gust velocities for the commuter aircraft and the larger commercial aircraft show no major differences.[9]

Figures 6 and 7 show the coincident gust load factor and airspeed during approach for half and full flaps along with gust V-n diagrams. The V-n diagrams in Figs. 6 and 7 are for illustration only and correspond to a gross weight of 14,500 lb and sea level altitude. The V-n diagrams are drawn using airspeed limits of 188 KIAS for flap detent position 1 (half) and 154 KIAS for flap detent position 2 (full), which are the operational placard limits.[16] Figures 6 and 7 indicate that the half-flap placard speed is only occasionally being slightly exceeded during approach with the flaps at half position and that the full-flap placard speed is being exceeded with the flaps at full a little more frequently. Similar data for half-flaps at departure showed no exceedances of the flap placard speeds. Operator practice

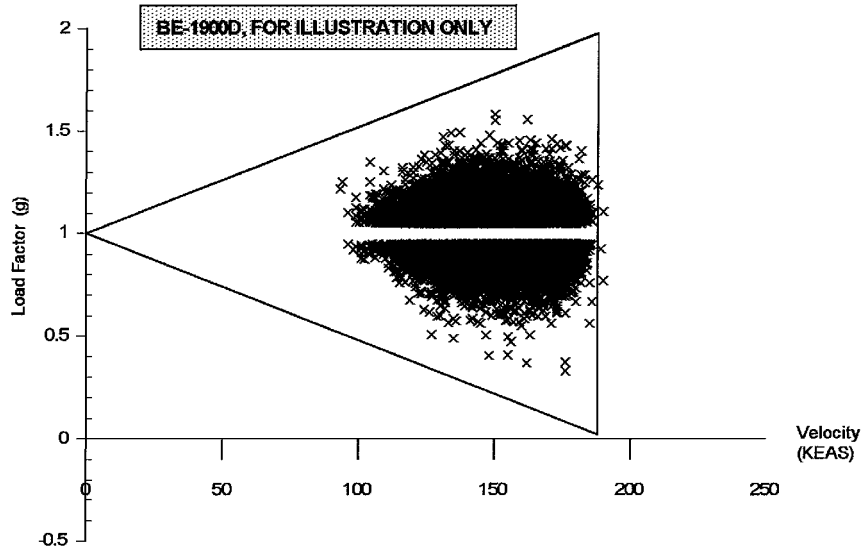

Fig. 6 Coincident gust load factor and speed during approach and V-n diagram, half-flaps.

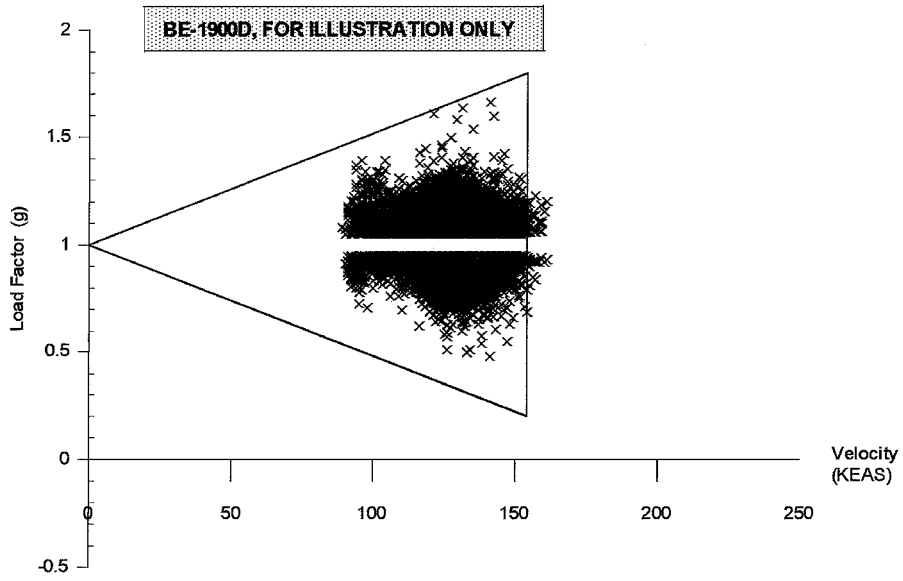

Fig. 7 Coincident gust load factor and speed during approach and V-n diagram for full flaps.

is that full flaps are never used for departure, and there was evidence that indications of full-flap usage during departure were the result of instrument malfunctioning. Hence, there are no reliable data for the use of full flaps at departure. Cases in which flap indicator malfunctions were evident were also removed from consideration for Figs. 6 and 7.

Figure 8 shows the maximum speed attained vs coincident altitude sorted by altitude band. Each data point represents the maximum airspeed attained within each 1000-ft band of altitude; therefore, the actual point is plotted for the maximum speed and the corresponding altitude where the maximum speed occurred. Also shown is the aircraft design operational speed line obtained from Ref. 16. This plot shows that this limit is occasionally being exceeded. These exceedances were found to occur during the cruise and descent phases of flight.

Figures 9 and 10 show the cumulative occurrences of maneuver load factor per 1000 hours and per nautical mile by pressure altitude for the combined climb, cruise, and descent flight phases. Departure and approach phases are not included because altitude above the airport is more pertinent than absolute altitude in these phases. Generally, the curves in these figures show that the most severe maneuvering occurs at lower altitudes, as might be expected. There is, nonetheless, an anomalous bulge for the positive incremental load factor for the highest altitude band. However, it must be remembered that these statistics may not be stabilized as a result of the sample size.

Earlier it was shown in Fig. 4 that the design gust spectra for twin-engine aircraft in general usage given in Ref. 13 are more severe than what the present data indicate. Reference 13 does not specify the method for determining the incremental maneuver design limit load factor. Therefore, this load factor was calculated in accordance with the approach specified in FAR 23.337 using the maximum takeoff gross weight of 16,950 lb. Figure 11 shows a similar comparison for incremental maneuver load factor. These data show that there is less difference between the maneuvering spectra in Ref. 13 and the present data than there is for the gust spectra presented earlier in Fig. 4. Though, the present data actually show a higher frequency of occurrence at the lower load factors.

Comparisons of usage were made between data recorded on other commuter aircraft and other published small aircraft data. Figure 12

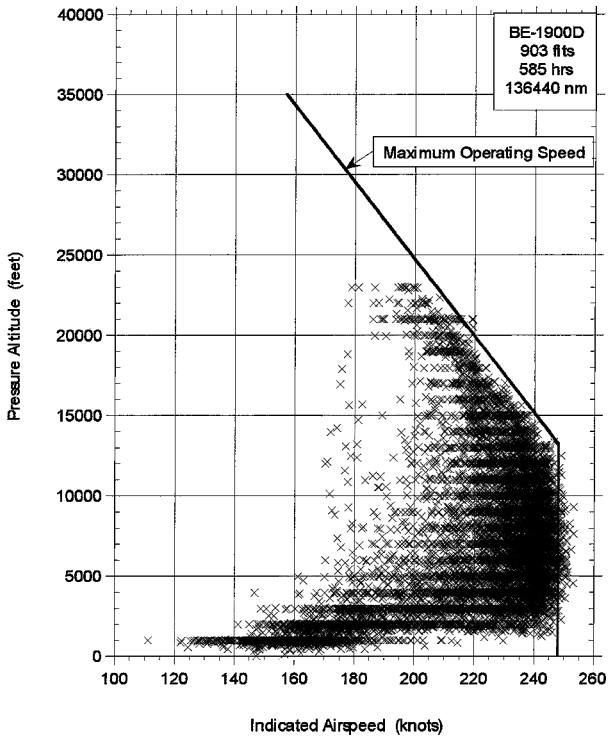

Fig. 8 Maximum speed and coincident altitude (all flight phases).

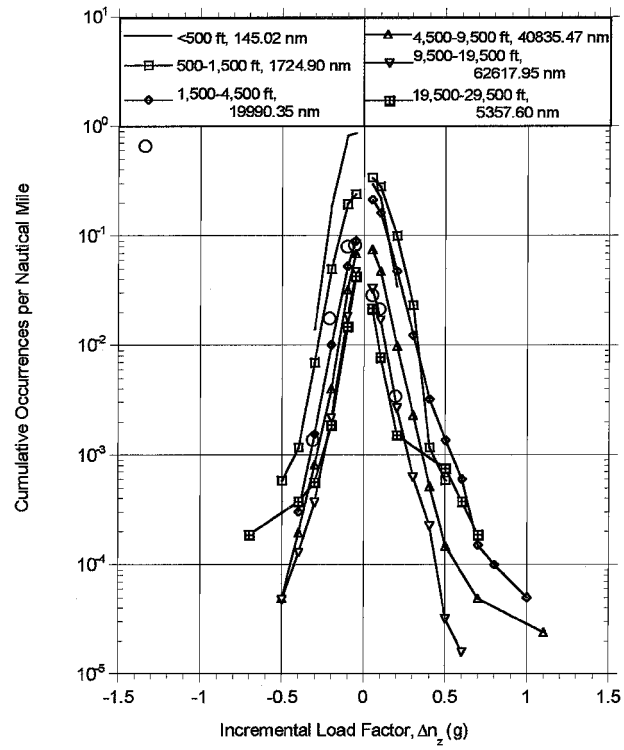

Fig. 10 Cumulative occurrences of incremental maneuver load factor per nautical mile by pressure altitude (combined climb, cruise, and descent phases).

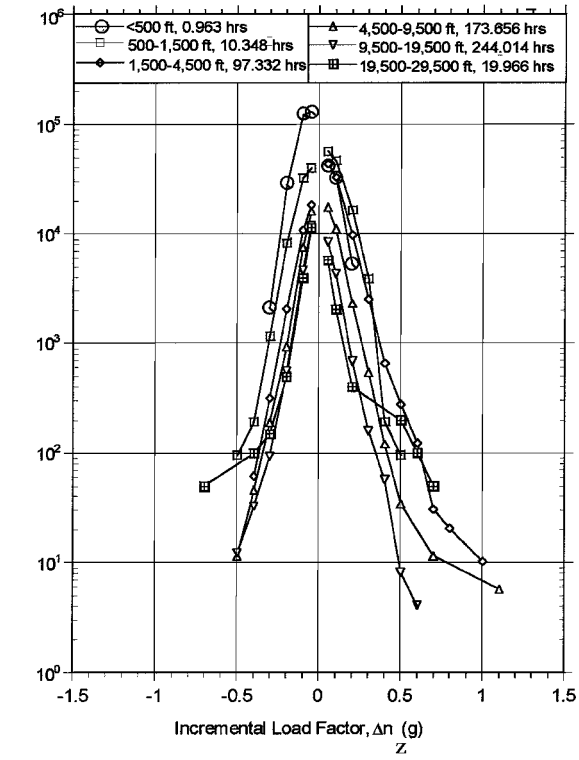

Fig. 9 Cumulative occurrences of incremental maneuver load factor per 1000 hours by pressure altitude (combined climb, cruise, and descent phases).

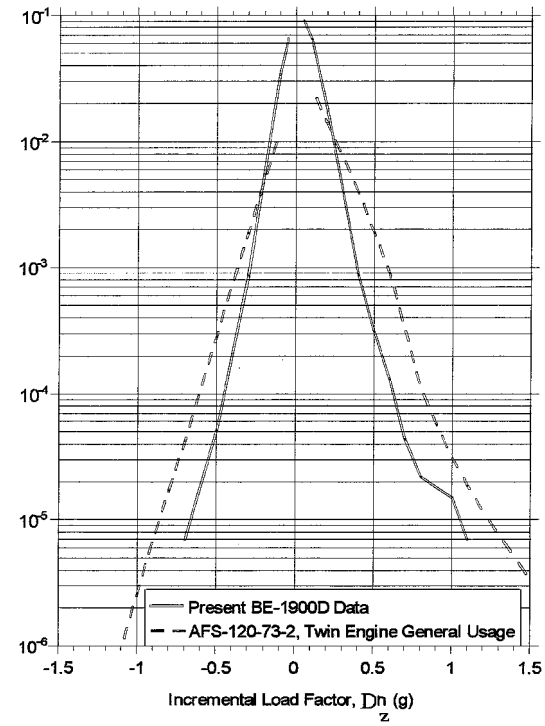

Fig. 11 Comparison of cumulative occurrences of incremental maneuver load factor per nautical mile, present data and AFS-120-73-2.

provides a comparison of the relative severity of vertical load factor for gust and maneuver combined between five commuter-type aircraft: the BE-1900D, the Canadair Challenger CL-601, and the DeHavilland Dash-8 aircraft (Ref. 2), the Fokker F-27 (Ref. 5), and the Fairchild/Dornier 328 (Ref. 8). The spectra from Ref. 2 are for aircraft engaged in low-altitude operations and are similarly and understandably more severe than the spectra from Refs. 5 and 8, which are for general usage. It can be seen that the present spectra are most similar, and nearly identical, to the two general usage spectra as would be expected.

In Fig. 13 is shown a comparison between the present BE-1900D spectrum for combined maneuver and gust and similar spectra developed by the aircraft manufacturer.[17] The load spectra in Ref. 17 were developed based on Refs. 13 and 18–20. These results show the present total spectrum to be less severe than the two manufacturer-developed total spectra.

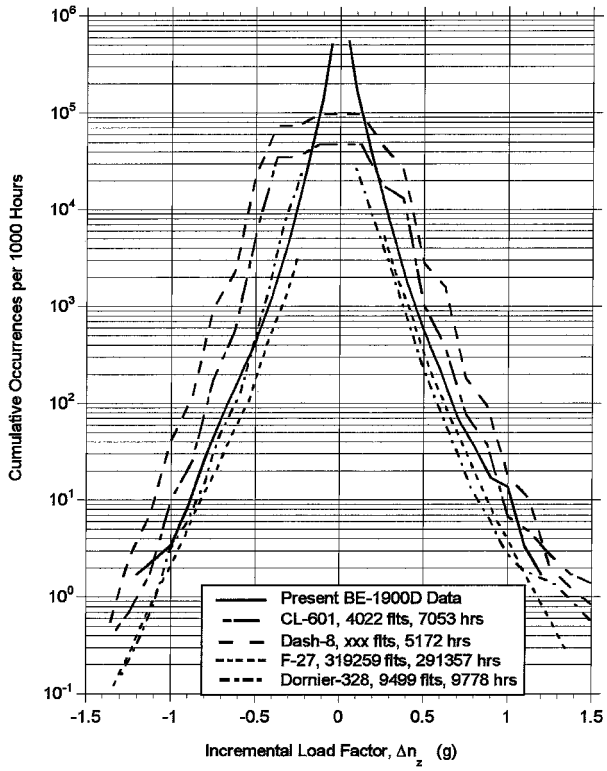

Fig. 12 Cumulative occurrences of incremental load factor per 1000 hours, present data, CL-601 and Dash-8, F-27, and Dornier-32 (combined flight phases).

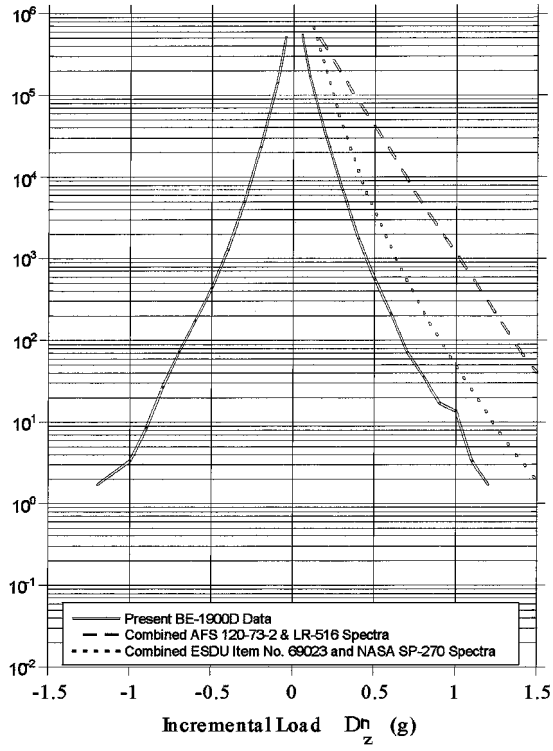

Fig. 13 Cumulative occurrences of incremental load factor per 1000 hours, present data and ref. 17 (combined flight phases).

Conclusions, Recommendations, Further Work

Comparisons of the BE-1900D statistical data with their operational limits and with data from other aircraft and published data revealed some interesting anomalies that require further study.

Maximum airspeed limits at various altitudes as defined in the aircraft's Type Certificate were being exceeded in some instances. Also, there were a few indications that flaps were being lowered in some instances at speeds in excess of the operational speed limits (placard speeds) associated with flap deployment.

Large differences in measured gust load factors between the commuter-type aircraft and the large transport aircraft were found but were accounted for by the differences in the load factor response of each aircraft.

The gust load factor spectra prescribed in AFS-120-73-2 for use in the fatigue design of general usage, twin-engine aircraft were considerably more severe than those indicated by the present data. The maneuver spectrum obtained from the present data is less severe than that prescribed by AFS-120-73-2 at the higher load factors, but more severe at the lower load factors. The total spectrum (maneuver and gust combined) developed by the aircraft manufacturer is more severe than that suggested by the present data. The generally more severe spectra used for design may explain why light aircraft designed under FAR-23 requirements exhibit useful lives in excess of those predicted using the AFS-120-73-2 design requirements. These results suggest a need for reevaluation of the fatigue design spectra.

Because calculating the derived gust velocity requires knowledge of the aircraft's gross weight and this information was not available for the BE-1900D, the average takeoff gross weight of 14,500 lb was assumed in order to do the calculations. It is recommended that future data include at least the aircraft takeoff and landing weight for improved accuracy of the derived gust velocities.

Some of the flight files that were received contained "bad" data that appeared to have resulted from the onboard instrumentation system. For example, the flap position indicator signal on two aircraft switched rapidly back and forth between half and full positions during the flight, the signal that indicted the direction of propeller rotation was reversed on several of the aircraft. Also, negative rpm values were measured on some flights. Although these problems can usually be found during editing, they cause disruptions to the normal processing activity and take a considerable amount of time to determine the cause of the problem and what course of action needed to be taken. Therefore, it is important that all onboard instrumentation be checked for proper installation, calibration, and sign convention prior to data recording during operational flights. This will ensure a maximum of useable data and will help to expedite the data editing and processing effort.

Additional instrumentation to record related parameters such as gross weight, fuel weight, lateral acceleration, and Mach number should be installed to provide more in-depth and accurate information to the user of these data. Also, the lack of a squat switch on the landing gear made establishing the exact moment of liftoff and touchdown difficult. This can lead to inaccuracies in the determination of the start of departure and landing phases and possibly the misplacement of load factor occurrences associated with these phases. Installation of a squat switch and these additional parameters are highly recommended.

Acknowledgments

The work reported in this paper was supported by Federal Aviation Administration Grant No. 98-G-018. The support and assistance of Thomas DeFiore and Terence Barnes of the FAA is gratefully acknowledged. Finally, aircraft operator assistance and cooperation, without which the collection of these data would not have been possible, is also gratefully acknowledged.

References

[1]Barnes, T., and DeFiore, T., "The New FAA Flight Loads Monitoring Program," 29th Aerospace Sciences Meeting, AIAA Paper 91-0258, Reno Nevada, Jan. 1991.

[2]David, G. M., "Analysis of Fatigue Loads Data Obtained from Transport Canada Challenger and Dash-8 Aircraft Engaged in Low-Level Flying Operations," Transport Canada, Rept. TP 11574, Ottawa, Canada, Nov. 1992.

[3]Locke, J. E., Smith, H. W., Gabriel, E., and DeFiore, T., "General Aviation Aircraft—Normal Acceleration Data Analysis and Collection Project," Dept. of Transportation, Rept. DOT/FAA/CT-91/20, FAA Technical Center, Atlantic City, New Jersey, Feb. 1993.

[4]Skinn, D., Miedlar, P., and Kelly, L., "Flight Loads Data for a Boeing

737-400 in Commercial Operation," Dept. of Transportation, Rept. DOT/FAA/AR-95/21, FAA Technical Center, Atlantic City, New Jersey, April 1996.

[5]de Jonge, J. B., and Hol, P. A., "Variation in Load Factor Experience of Fokker F-27 and F-28 Operational Acceleration Exceedance Data," Dept. of Transportation, Rept. DOT/FAA/AR-96/114, FAA Technical Center, Atlantic City, New Jersey, Dec. 1996.

[6]Rustenburg, J. W., Skinn, D., and Tipps, D. O., "Statistical Loads Data for Boeing 737-400 Aircraft in Commercial Operations," Dept. of Transportation, Rept., DOT/FAA/AR-98/28, FAA Technical Center, Atlantic City, New Jersey, Aug. 1998.

[7]Skinn, D., Tipps, D. O., and Rustenburg, J., "Statistical Loads Data for MD-82/83 Aircraft in Commercial Operations," Dept. of Transportation, Rept. DOT/FAA/AR-98/65, FAA Technical Center, Atlantic City, New Jersey, Feb. 1999.

[8]Brunbauer, R., Herbing, B., Hickethier, H., and Teske, R., "Results of the Dornier 328 Operational Loads Recording Campaign," *Proceedings of the 20th ICAF Symposium*, International Committee on Aeronautical Fatigue, Bellevue, Wshington, July 1999.

[9]Tipps, D. O., Skinn, D. A., Rustenburg, J. W., and Zeiler, T. A., "Statistical Loads Data for BE-1900D Aircraft in Commuter Operations," Dept. of Transportation, Rept. DOT/FAA/AR-00/11, FAA Technical Center, Atlantic City, New Jersey, April 2000.

[10]"Jane's all the World's Aircraft 1997–1998," Jane's Information Group, Coulsdon, Surrey, UK, p. 710.

[11]de Jonge, B., "Reduction of Incremental Load Factor Acceleration Data to Gust Statistics," Dept. of Transportation, Rept. DOT/FAA/AR-94/57, FAA Technical Center, Atlantic City, New Jersey, Aug. 1994.

[12]Rustenburg, J. W., Skinn, D., and Tipps, D. O., "An Evaluation of Methods to Separate Maneuver and Gust Load Factors from Measured Acceleration Time Histories," Dept. of Transportation, Rept. DOT/FAA/AR-99/14, FAA Technical Center, Atlantic City, New Jersey, April 1999.

[13]"Fatigue Evaluation of Wing and Associated Structures on Small Aircraft," Dept. of Transportation, Rept. AFS-120-73-2, FAA Technical Center, Atlantic City, New Jersey, May 1973.

[14]Nicolai, L. M., *Fundamentals of Aircraft Design*, METS, Inc., San Jose, CA, 1975.

[15]Hoblit, F. M., Paul N., Shelton, J. D., and Ashford, F. A., "Development of a Power Spectral Gust Design Procedure for Civil Aircraft," Federal Aviation Agency, TR FAA-ADS-53, Jan. 1966.

[16]Federal Aviation Administration Type Certificate Data Sheet Number A-24CE, Revision 68, Raytheon Aircraft Company, Wichita, KS, March 1991.

[17]Smith, J., "Structural Airworthiness of New and Aging Aircraft: Load Spectra Derivation and Measurement," Society of Automotive Engineers, Paper 931257, Wichita, Kansas, May 1993.

[18]Sewell, R. T., "Analysis of Flight Loads During Low-Altitude Pipeline Patrol Operations," National Research Council of Canada, Aeronautical Rept. LR-516, Transport Canada, Ottawa, Canada, Dec. 1968.

[19]"Average Gust Frequencies Subsonic Transport Aircraft," Engineering Sciences Data Item 69023, Royal Aircraft Establishment, Engineering Sciences Data Unit, London, U.K., May 1972.

[20]Jewel, J. W., Jr., "Progress Report on the NASA V-G/VGH General Aviation Program," NASA SP-270, May 1971.